Novel Polymer Electrolytes Based on Amorphous Poly(ether−ester)s Containing 1,4,7-Trioxanonyl Main Chain Units. Ionic Conductivity versus Polymer Chain Mobility

I. J. A. Mertens,[†] M. Wübbenhorst,[‡] W. D. Oosterbaan,[†] L. W. Jenneskens,*[,†] and J. van Turnhout[‡]

Debye Institute, Department of Physical Organic Chemistry, Utrecht University, Padualaan 8, 3584 CH Utrecht, The Netherlands, and Department of Polymer Technology, Faculty of Applied Sciences, Delft University of Technology, Julianalaan 136, 2628 BL Delft, The Netherlands

Received December 8, 1998; Revised Manuscript Received March 2, 1999

ABSTRACT: Melt condensation of 1,5-bis(9-hydroxy-1,4,7-trioxanonyl)naphthalene (**2**) with bis-acid chlorides, adipoyl chloride (**3a**), terephthaloyl chloride (**3b**), and 3,6,9,12-tetraoxatetradecane bis-acid chloride (**3c**), respectively, gives amorphous linear poly(ether−ester)s **1a**−**c**, which contain 1,4,7-trioxanonyl (triethylene glycol) units at regular intervals in their main chain. Solid polymer electrolytes were prepared by mixing THF solutions of either $LiClO_4$ with **1a**−**c** or $NaClO_4$ with **1b**. The polymer electrolytes containing $LiClO_4$ are fully amorphous, whereas in the case of $NaClO_4$ and Na^+/**1b** ratios larger than 0.125, crystalline $NaClO_4$ is present. Despite the fact that the 1,4,7-trioxanonyl moieties in **1a**−**c** are shorter than the minimum required for complete solvation of Li^+ and Na^+, dielectric relaxation spectroscopy shows that the solid polymer electrolytes Li^+/**1a**, Li^+/**1b**, and Li^+/**1c** possess ionic conductivities of $\sigma = 3.2 \times 10^{-5}$, 1.9×10^{-6}, and even 1×10^{-4} S cm^{-1}, respectively, at 368 K. A Vogel−Tammann−Fulcher (VTF) analysis of the ionic conductivity σ and the relaxation time of the α-relaxation revealed a strong relationship between σ and the relaxation behavior of the chain segments. By means of a fine structure analysis of the activation energy, the dielectric α-process around the glass transition was closely studied in the absence and presence of dissolved $LiClO_4$ (**1a**−**c**) or $NaClO_4$ (**1b**). From the highest apparent activation energy the T_g was determined and found to agree very well with values from DSC. In addition, the fractional free volume at T_g was quantified. It increases with increasing amount of dissolved salt; this becomes in particular clear from the fine structure analysis. Dielectric spectroscopy at $T < T_g$ showed the presence of three secondary relaxations (γ, β_1, β_2), of which β_1 and β_2 strongly overlap. Two of them are assigned to local relaxations involving either free (γ) or coordinated (β_2) EO sequences, resulting in a decrease or increase of the relaxation strength with salt concentration, respectively. Molecular modeling supports the idea that the β_2 process arises from a chemical relaxation by the temporary breaking up and remaking of at least one O−Li^+ coordination bond within the tetrahedral polymer−cation complex. The third (β_1) relaxation is in particular active in weakly complexed samples exposed to ambient humidity, suggesting a local motion involving the ester moieties.

Introduction

Solvent-free solid polymer electrolytes with ionic conductivities σ in the range 10^{-5}−10^{-2} S cm^{-1} at ambient or moderately elevated temperatures receive considerable attention.[1−4] In these materials inorganic salts are dissolved by cation coordination, and short-range ionic motion has to occur by local liquidlike polymer segmental motions.[5] Hence, for the preparation of suitable ion-conducting materials the polymer host has to fulfill several requirements. (1) It has to solvate inorganic salts, such as LiX and NaX (X = ClO_4^- or $CF_3SO_3^-$). This is accomplished by incorporation of $-(CH_2CH_2X)_n-$ units, with X being O, N, or S. The solubility of the inorganic salts is primarily controlled by their lattice energy, which has to be compensated for by cation coordination. (2) Since for ion transport in a solid polymer electrolyte segmental motion of the chains is a prerequisite, they have to be amorphous materials with preferably a low glass transition temperature (T_g). (3) Finally with regard to their application, the polymer electrolytes have to be both mechanically and electrochemically stable. Poly(ethylene oxide) (PEO), first explored by Wright[6] and Armand,[7] is the archetypal material. A serious drawback is its propensity to give crystalline salt/polymer complexes in which ion transport is impaired. To circumvent this problem, PEO derived polymer networks and blends, comb-branch polymers containing pending oligo(ethylene glycol) side chains, and hyperbranched poly(ethylene glycols) salt/polymer complexes have been prepared and evaluated.[1,8−10]

In a recent communication we reported the synthesis of an amorphous poly(ether−ester) containing 1,4,7-trioxanonyl (triethylene glycol) segments (**1a**) at regular intervals in its main chain using a melt condensation procedure (Scheme 1).[11] Although only triethylene glycol units are present, which are shorter than the minimum required for complete intrachain solvation, viz. coordination, of Li^+ cations, dielectric spectroscopy gave ionic conductivities σ of up to 3.3×10^{-5} S cm^{-1} K for Li^+/**1a** salt/polymer complexes at 368 K.

Here we report on the ionic conductivity properties of solid polymer electrolytes derived from related amorphous linear poly(ether−ester)s (**1b**,**c**). For **1c** the introduction of additional ethylene glycol moieties in the bis-acid moiety, viz. **3c** (vide infra), gave an increase in σ of up to 1×10^{-4} S cm^{-1} at 368 K (dissolved inorganic

* Corresponding author. Tel +31 302533128; Fax +31 302534533; E-mail jennesk@chem.uu.nl.
[†] Utrecht University.
[‡] Delft University of Technology.

10.1021/ma981901j CCC: $18.00
Published on Web 04/24/1999

Table 1. Selected Data for Poly(ether−ester)s 1a−c Prepared by Melt Polycondensation

polymer	monomers	yield [%]	M_w [SEC]	D [M_w/M_n]	T_g (T_{onset}/T_{offset}) [K]	TGA(N_2) (T_{onset}/T_{max})[a] [K]	$T_{(5\%\ wt\ loss)}$ [K]	$T_{(100\%\ wt\ loss)}$ [K]
1a	**2/3a**	75	4.8×10^4	1.99	$T_g = 252.8$ (251/255)	598/683	637	900
1b	**2/3b**	65	1.6×10^4	1.80	$T_g = 282.5$ (280/285)	608/713	664	1120
1c	**2/3c**	80	2.5×10^4	2.05	$T_g = 251.1$ (250/253)	478/675	605	898

[a] T_{max} taken from first-derivative curve.

Scheme 1. Synthesis of Poly(ether−ester)s 1a−c by Melt Condensation

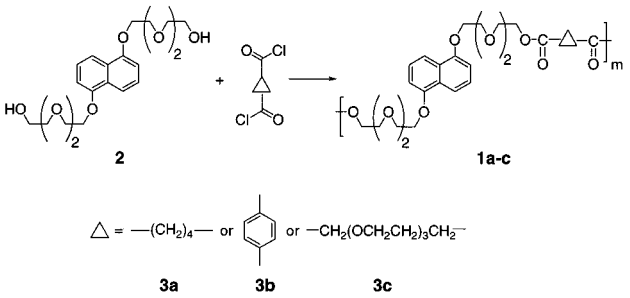

salt $LiClO_4$). A Vogel−Tammann−Fulcher (VTF) analysis of the σ data confirms the (expected) strong interrelation between σ and the relaxation behavior of the polymer chain segments. By VTF fitting, William−Landel−Ferry (WLF) parameters and free volume constants are derived and discussed. The dissolution of $LiClO_4$ and $NaClO_4$ leads to an increase in free volume in particular for **1a,b**. For a more detailed elucidation, the segmental relaxation behavior of the solid polymer electrolytes derived from **1a**−**c** was studied using a fine structure analysis of the activation energy.

Results and Discussion

Polymer Synthesis. Poly(ether−ester)s **1a**−**c** were prepared by melt condensation[11,12] of 1,5-bis(9-hydroxy-1,4,7-trioxanonyl)naphthalene (**2**) with the bis-acid chlorides, adipoyl chloride (**3a**), terephthaloyl chloride (**3b**), and 3,6,9,12-tetraoxatetradecane bis-acid chloride (**3c**), respectively (Scheme 1). The bis-acid moiety **3c** (See Experimental Section) contains additional −CH_2−CH_2−O− moieties, which can also participate in cation complexation. The high molecular weight fraction of **1a**−**c** was isolated and purified from both linear and cyclic oligomers[13] by precipitation in CH_3OH (**1a**−**c** highly viscous oils, Table 1). ^1H and ^{13}C NMR and FT-IR spectroscopy revealed that neither hydroxy nor carboxylate end groups were discernible. Size exclusion chromatography (SEC) gave molecular weight distributions M_w ($D = M_w/M_n$) for precipitated **1a**−**c** in the range 1.6×10^4 (1.80) to 7.9×10^4 (2.56) [Table 1].[14] The thermal stability of **1a**−**c** was evaluated using thermogravimetry under a N_2 atmosphere [TGA(N_2)]. Whereas no weight loss is found at $T < 600$ K for **1a**,**b**,[11] weight loss sets in already at 478 K for **1c** (see Supporting Information). The latter result is attributed to a decrease in thermal stability of the covalently incorporated **3c**; according to TGA(N_2), **3c** starts losing weight at 370 K. Hence during the preparation of **1c**, the high-temperature treatment at the end of the melt polycondensation procedure was omitted (see Experimental Section).

Polarization microscopy and differential scanning calorimetry (DSC) showed that **1a**−**c** are amorphous

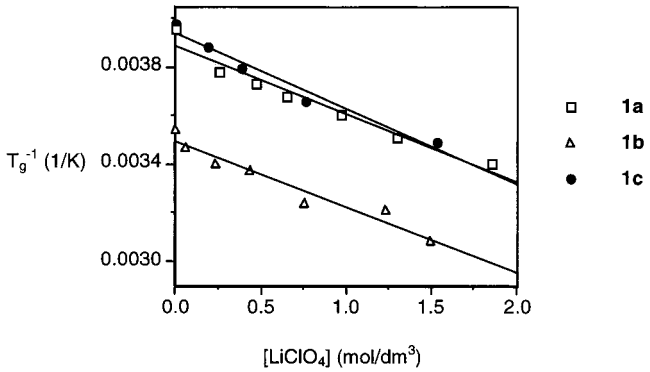

Figure 1. T_g(DSC)$^{-1}$ versus $LiClO_4$ concentration (mol of Li^+ per dm^3 polymer) for solid polymer electrolytes Li^+/**1a**, Li^+/**1b**, and Li^+/**1c**.

with glass transition temperatures [T_g(DSC)] below ambient temperature; no melt/crystallization processes were discernible in subsequent heating and cooling runs (Table 1). In the case of **1a** and **1c** T_g(DSC) is lowered by ca. 30 K compared to that of **1b**. This agrees with the change in rigidity in going from an adipoyl (**1a**; aliphatic) and 3,6,9,12-tetraoxatetradecanoyl bis-acid unit (**1c**) to a terephthaloyl (aromatic) unit (**1b**).[15] Further evidence of the amorphous character of **1a**−**c** was obtained by wide-angle X-ray diffraction (WAXD); curves of the intensity vs 2θ show only two broad halos at 2θ values ranging from 5° to 60°, in agreement with the absence of three-dimensional crystalline order (see Supporting Information).

Solid Polymer Electrolytes Derived from 1a−**c.** To obtain solid polymer electrolytes, THF solutions of the polymers **1a**−**c** and $LiClO_4$ were mixed followed by slow evaporation of the solvent in a dry N_2 atmosphere. Different molar ratios between the cation and the polymer repeat unit were used. From **1b** polymer electrolytes with $NaClO_4$ were also prepared (see Experimental Section). Due to differences in polymer chain composition, a salt concentration of 1.0 for **1a,b** corresponds to a salt/polymer complex with 10 oxygen atoms (8 ether-like and 2 ester-like) per cation, whereas for **1c** 14 oxygen atoms (12 ether-like and 2 ester-like) are available per cation. The amorphous character of the $LiClO_4$ containing salt/polymer complexes was established using DSC and WAXD. To assess whether physisorbed water is present in the solid polymer electrolytes, all samples were carefully checked using solid-state FT-IR spectroscopy; no physisorbed water could be detected.

In the $LiClO_4$/polymer complex series, T_g(DSC) increases concomitant with increasing Li^+ concentration. Linear relationships are found between the inverse of T_g and the Li^+ cation concentration expressed in moles of Li^+ cations per dm^3 polymer [r^2: Li^+/**1a**, 0.96; Li^+/**1b**, 0.95; and Li^+/**1c**, 0.97 (Figure 1)]. This suggests that the 1,4,7-trioxanonyl (triethylene glycol) segments apparently participate in interchain, noncovalent physical

(ion-dipole) cross-linking in the presence of metal cations, which will restrict the segmental motions of the polymer. Since the slopes are nearly identical (Li^+/**1a**, -2.80×10^{-4} dm^3 mol^{-1} K^{-1}; Li^+/**1b**, -2.77×10^{-4} dm^3 mol^{-1} K^{-1}; Li^+/**1c**, -3.12 dm^3 mol^{-1} K^{-1}),[16] differences in hydrocarbon architecture of **1a**, **1b**, and **1c**, viz. the presence of an aliphatic, aromatic, and ethylene glycol containing bis-acid moiety, only moderately affects Li^+ complexation. The slopes are in line with those found for isocyanate cross-linked PEO networks (-2.7×10^{-4} dm^3 mol^{-1} K^{-1}).[9] This suggests that, independent of the polymer hydrocarbon architecture, the increase of T_g upon addition of Li^+ cations is due to Li^+ complexation by the ethylene glycol sequences.

In contrast, the polymer electrolyte series $NaClO_4$/**1b** shows a different DSC behavior with $NaClO_4$ loading (see Supporting Information). Whereas T_g(DSC) initially increases up to Na^+/**1b** 0.125, any additional $NaClO_4$ does not affect T_g. The leveling off T_g above Na^+/**1b** 0.125 indicates that $NaClO_4$ is not properly dissolved, and so no increase in polymer chain stiffening due to (enhanced) interchain physical cross-linking[11] occurs. WAXD measurements of the sample Na^+/**1b** 1.0 gave sharp lines superpositioned on top of broad halos (see Supporting Information). A comparison with available WAXD data for crystalline $NaClO_4$ (orthorhombic[17] and cubic[18]) revealed unambiguously that orthorhombic $NaClO_4$ was present. Since the polymer electrolytes were prepared by mixing THF solutions of **1b** and $NaClO_4$, crystallization has evidently occurred upon removal of the solvent (see Supporting Information).[19]

It is noteworthy that the T_g(DSC) value of Na^+/**1b** 0.125 (295.7 K) is higher than that of the related Li^+/**1b** 0.125 (289.1 K) polymer electrolyte. This suggests that different coordination numbers are required for the dissolution of Na^+ and Li^+. For crystalline salt/PEO complexes it is documented that Na^+ requires more coordination sites than Li^+ (coordination numbers: Na^+, 6; Li^+, 5).[20] If these results are also applicable for our solid polymer electrolytes, Na^+ will restrict the chain segment mobility to a larger extent than Li^+.

Ionic Conductivity of Solid Polymer Electrolytes Derived from 1a−c. The ion-conducting properties of solid polymer electrolytes Li^+/**1a**,[11] Li^+/**1b**, Na^+/**1b**, and Li^+/**1c** were determined as a function of temperature and metal cation concentration using dielectric spectroscopy (see Experimental Section: Dielectric Thermal Analysis; Sample Preparation).[21] Dissolution of $LiClO_4$ leads to an increase in ionic conductivity by 3 orders of magnitude, viz. from $\sigma = 2.6 \times 10^{-8}$ S cm^{-1} for pristine **1a** to 3.3×10^{-5} S cm^{-1} for Li^+/**1a** 0.25 at 368 K. For Li^+/**1b** polymer electrolytes the increase of σ is similar (**1b**, 3.1×10^{-9} S cm^{-1}; Li^+/**1b** 0.25, 1.9×10^{-6} S cm^{-1} at 368 K). It is noteworthy, however, that σ for the Li^+/**1b** series is lower than that of the related Li^+/**1a** series.[22] For the latter σ varies by less than a factor of 4 at 368 K. In fact, the solid polymer electrolyte containing only a moderate amount of dissolved Li^+ possesses the highest σ value; the same applies to the Li^+/**1b** series. Whereas σ at 368 K for Li^+/**1b** 0.03 is 2.5×10^{-7} S cm^{-1}, the σ values for Li^+/**1b** 0.125 and 0.25 are comparable, i.e., $\sigma = 1.1 \times 10^{-6}$ S cm^{-1} and $\sigma = 1.9 \times 10^{-6}$ S cm^{-1}, respectively. The σ value of **1c** equals 9.4×10^{-7} S cm^{-1} at 368 K, which is higher than that found for pristine **1a** and **1b**. It is likely that **1c** already contains some Na^+ as an impurity. Note that for **3c** the bis-sodium salt of 3,6,9,12-tetraoxadecatetradecane bis-acid has to be converted with excess oxalyl chloride, giving NaCl as an additional product (see Experimental Section). The Li^+/**1c** polymer electrolytes already show enhanced σ values with respect to their related Li^+/**1a** and Li^+/**1b** analogues. Hence, an increase in the number of ethylene glycol moieties in the polymer main chain leads to an improvement of σ by nearly an order of magnitude (Li^+/**1a** 0.25, 3.2×10^{-5} S cm^{-1}; Li^+/**1c** 0.50, 1×10^{-4} S cm^{-1} at 368 K). The σ values compare favorably with those found for other PEO derived polymer electrolytes: $LiClO_4$/PEO (6×10^{-6} S cm^{-1} at 312 K),[23] NaI/PEO (10^{-6} S cm^{-1} at 298 K),[24] oxymethylene linked $LiClO_4$/PEO (5×10^{-5} S cm^{-1} at 298 K),[25] $LiClO_4$/PEO blends (10^{-5} S cm^{-1} at 298 K),[26] and $LiClO_4$/hyperbranched poly(ethylene glycol) complexes (10^{-5} S cm^{-1} at 303 K).[10]

For all solid polymer electrolyte series, the temperature dependence of σ is non-Arrhenius such as and should be analyzed using a Vogel−Tammann−Fulcher (VTF)[27] type equation (eq 1):

$$\sigma(T) = \sigma_0 \exp\left\{-\frac{E_v}{R(T - T_v)}\right\} \qquad (1)$$

in which R and T_v represent the gas constant [8.31 J mol^{-1} K^{-1}] and the Vogel scaling temperature, while σ_0 and E_v [kJ mol^{-1}] denote the ultimate conductivity and Vogel "activation" energy. The fit results for the polymer electrolyte series Li^+/**1a**, Li^+/**1b**, and Li^+/**1c** are presented in Figures 2−4 (lines) and in Tables 2−4, respectively. For comparison, the conductivity curves of the Li^+/**1a** series are also presented as a function of the reduced temperature $T - T_v$; linear graphs are obtained (Figure 5). Although the high-temperature σ values of the Li^+/**1a** and Li^+/**1b** series are of similar magnitude, an increase of the temperature coefficient d log σ/d[1/($T - T_v$)] $\propto E_v$ is found upon increasing the Li^+ content (Tables 2 and 3). Contrary to the results for the Li^+/**1a** and Li^+/**1b** series, the Vogel "activation" energy parameter E_v of the Li^+/**1c** series does not increase with increasing Li^+ content (see also Table 4).

The accuracy of the VTF fits over a wide temperature range ($T_g + 5$ K $\leq T \leq T_g + 100$ K) demonstrates the strong relation between σ and chain segment mobility.[28] Additional support for this conjunction was obtained by fitting the mean relaxation time τ_α of the α-relaxation process taken from the dielectric loss peak with a VTF equation $\ln \tau_\alpha = \ln \tau_0 - E_v/R(T - T_v)$ (see Figures 2b and 3b).[29] The VTF parameters (T_v and E_v) of the dielectric relaxation process (peak frequency $f_\alpha = 1/2\pi\tau_\alpha$) correspond quite well to those derived for the conductivity data.[11] The temperature dependence of σ and τ_α will be discussed in more detail in a forthcoming paper.[30]

The strong coupling between the segmental motion and the ionic conductivity can be rationalized in different ways. Taking into account that σ depends on the charge carrier concentration n_i, the charge q_i, and the charge carrier mobility μ_i (eq 2),

$$\sigma = \sum_i n_i q_i \mu_i \qquad (2)$$

we conceive that the chain mobility controls the generation (release of coordinated Li^+) and the mobility of both cations (Li^+) and anions (ClO_4^-). Under the likely assumption that μ_i is related to the free volume,[31] the

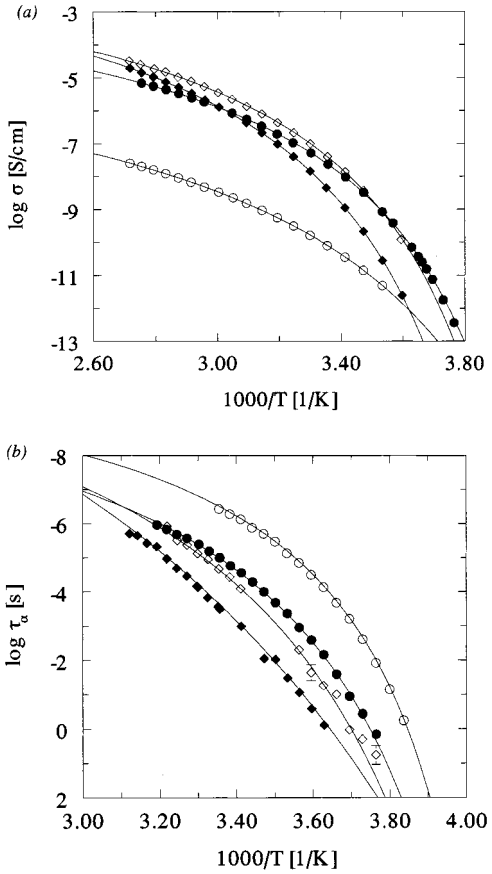

Figure 2. Log σ versus 1000/T (a) and Log τ_α (s) versus 1000/T (b) for solid polymer electrolytes Li^+/**1a**: (○) **1a**, (●) Li^+/**1a** 0.125, (□) Li^+/**1a** 0.25, and (■) Li^+/**1a** 0.50.

temperature dependence $\sigma(T)$ can be described by the William−Landel−Ferry (WLF) equation (eq 3):[32]

$$\log\left(\frac{\sigma(T)}{\sigma(T_g)}\right) = \frac{C_1(T - T_g)}{C_2 + T - T_g} \qquad (3)$$

in which $C_1 = 17.4$ and $C_2 = 51.6$ K represent "universal" constants for free volume relaxations in amorphous polymers. T_g is the calorimetrically determined glass transition temperature [T_g(DSC)] and σ_{T_g} denotes the conductivity at T_g.[33,34] Note that eqs 1 and 3 are equivalent and can be transformed into each other using the relations $C_2 = T_g - T_v$, $C_1 = E_v/(2.303RC_2)$, and $\log \sigma_{T_g} = \log \sigma_0 - C_1$. The WLF parameters C_1 and C_2 can be related to the free volume by $f(T_g) = b/(2.303C_1)$ and $\alpha_f = f(T_g)/C_2$, where $f(T_g)$ and α_f denote the fractional free volume at T_g and its temperature coefficient, respectively, while b is a constant. Taking $b = 1$,[31,32] α_f and $f(T_g)$ were calculated (Tables 2−4). The analysis based on the conductivity data shows a significantly higher fractional free volume at T_g for the polymer electrolyte series Li^+/**1a** and Li^+/**1b**. By contrast, the extrapolated fractional free volume for conduction at T_g [$f(T_g)$] in the Li^+/**1c** series does not increase with increasing Li^+ content but remains constant. Pristine **1a**, **1b**, and **1c** possess $f(T_g)$ values for conduction of 0.036, 0.037, and 0.037, respectively, which are significantly higher than those predicted using the "universal" free volume constants [$f(T_g) \approx 0.025$] for main chain relaxations.

The concentration of mobile Li^+ cations might vary, because it is conceivable that Li^+ complexation will be affected by changes in the segmental chain motion. Our observation that with increasing Li^+ content no significant further increase in σ occurs suggests that for the $LiClO_4$ complexes of **1a,b** $\mu_i(Li^+)$ is hindered by the reduction of the number and length of flexible ethylene glycol sequences due to (temporary) physical cross-linking. So in contrast to the Li^+/**1c** series, σ is mainly limited by a hindered Li^+ mobility [μ_i (eq 2)], rather than by a limited amount of free volume present.

Also for the Na^+/**1b** complexes, σ increases substantially with respect to that of the pristine **1b** [300 K, 3.5×10^{-13} S cm^{-1}; 368 K, 3.2×10^{-9} S cm^{-1}; Na^+/**1b** 0.5, 300 K, 1×10^{-12} S cm^{-1}; 368 K, 1.4×10^{-6} S cm^{-1}]. It is clearly comparable to that of the Li^+/**1b** polymer

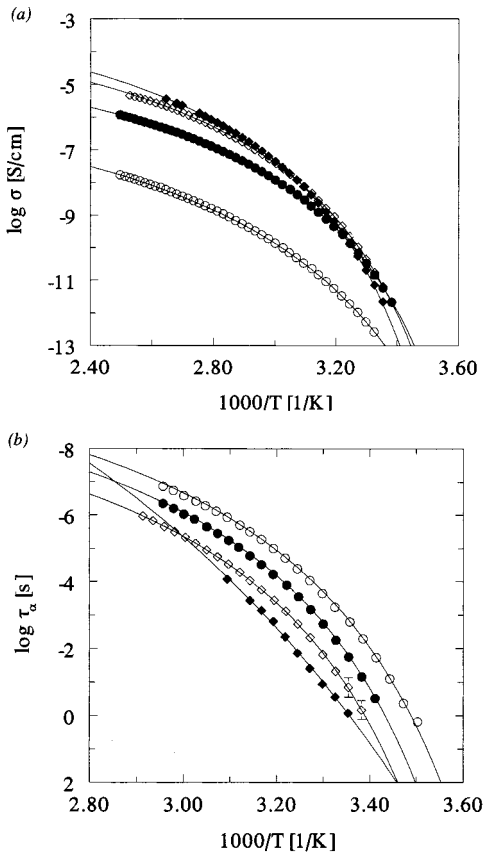

Figure 3. Log σ versus 1000/T (a) and log τ_α (s) versus 1000/T (b) for solid polymer electrolytes Li^+/**1b**: (○) **1b**, (●) Li^+/**1b** 0.03, (□) Li^+/**1b** 0.125, and (■) Li^+/**1b** 0.25.

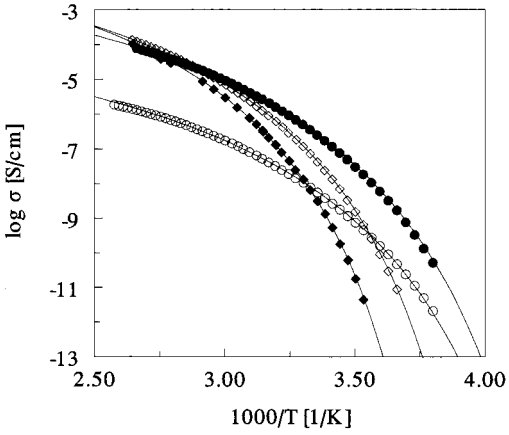

Figure 4. Log σ versus 1000/T for solid polymer electrolytes Li^+/**1c**: (○) **1c**, (●) Li^+/**1c** 0.125, (□) Li^+/**1c** 0.50, and (■) Li^+/**1c** 1.0.

Table 2. VTF and WLF Parameters Derived from (a) Conductivity and (b) Relaxation Time Based Fits for Solid Polymer Electrolytes Li^+/1a

		VTF parameters			WLF free volume parameters				
sample	T_g(DSC)[a] [K]	log σ_0	E_v [kJ mol^{-1}]	T_v [K]	log σ_{T_g}	C_1	C_2 [K]	$f(T_g)$	$\alpha_f \times 10^4$ [K^{-1}]
(a) VTF Parameters Determined from Conductivity Fits									
Li^+/**1a** 0.00	253.7	−2.6	8.58	215.8	−14.6	12.0	37.2	0.036	9.7
Li^+/**1a** 0.125	265.2	−0.6	6.41	231.1	−10.5	9.9	33.9	0.044	12.9
Li^+/**1a** 0.25	268.4	0.2	6.90	233.4	−10.2	10.4	34.6	0.042	12.1
Li^+/**1a** 0.50	277.1	0.6	8.25	235.6	−9.8	10.4	41.4	0.042	10.1
(b) VTF Parameters Determined from the α-Relaxation Time τ_α									
Li^+/**1a** 0.00	253.7	−10.7	5.00	235.5	4.2	14.9	17.5	0.029	16.6
Li^+/**1a** 0.125	265.2	−10.7	7.33	231.0	0.4	11.1	34.4	0.039	11.3
Li^+/**1a** 0.25	268.4	−12.1	10.32	225.8	0.7	12.8	42.2	0.034	8.1
Li^+/**1a** 0.50	277.1	−16.8	27.40	189.3	−0.5	16.3	87.7	0.027	3.0

[a] T_g, DSC was also determined for Li^+/**1a** 0.33 (272 K), Li^+/**1a** 0.67 (285 K), and Li^+/**1a** 1.00 (294 K) [Figure 1].

Table 3. VTF and WLF Parameters Derived from (a) Conductivity and (b) Relaxation Time Based Fits for Solid Polymer Electrolytes Li^+/1b

		VTF parameters			WLF free volume parameters				
sample	T_g(DSC)[a] [K]	log σ_0	E_v [kJ mol^{-1}]	T_v [K]	log σ_{T_g}	C_1	C_2 [K]	$f(T_g)$	$\alpha_f \times 10^4$ [K^{-1}]
(a) VTF Parameters Determined from Conductivity Fits									
Li^+/**1b** 0.00	282.3	−2.9	8.74	241.1	−14.6	11.7	39.0	0.037	9.5
Li^+/**1b** 0.03	287.6	−1.5	6.85	251.5	−12.2	10.7	33.6	0.041	12.2
Li^+/**1b** 0.125	289.1	−0.6	7.45	253.0	−11.7	11.1	35.2	0.039	11.1
Li^+/**1b** 0.25	296.2	−0.1	7.66	256.5	−10.2	10.1	39.8	0.043	10.8
(b) VTF Parameters Determined from the α-Relaxation Time τ_α									
Li^+/**1b** 0.00	282.3	−11.8	8.10	250.8	1.6	13.4	31.5	0.032	10.3
Li^+/**1b** 0.03	287.6	−11.3	7.81	255.2	1.3	12.6	32.4	0.035	10.6
Li^+/**1b** 0.125	289.1	−10.7	7.81	256.9	2.0	12.7	32.2	0.034	10.6
Li^+/**1b** 0.25[b]	296.2								

[a] T_g(DSC) was also determined for Li^+/**1b** 0.40 (308.7 K) and Li^+/**1b** 0.80 (324.0 K) [Figure 1]. [b] See ref 29.

Table 4. VTF and WLF Conductivity-Based Fit Parameters Derived for Solid Polymer Electrolytes Li^+/1c

		VTF parameters			WLF free volume parameters				
sample	T_g(DSC)[a] [K]	log σ_0	E_v [kJ mol^{-1}]	T_v [K]	log σ_{T_g}	C_1	C_2 [K]	$f(T_g)$	$\alpha_f \times 10^4$ [K^{-1}]
Li^+/**1c** 0.00	251.8	−1.3	8.03	213.7	−13.0	11.7	35.8	0.037	10.3
Li^+/**1c** 0.125	257.6	0.7	8.58	212.6	−10.6	11.3	39.6	0.038	9.6
Li^+/**1c** 0.50	273.4	1.2	8.61	229.0	−10.5	11.7	38.4	0.037	9.6
Li^+/**1c** 1.00	286.8	1.3	8.58	240.8	−10.2	11.5	39.0	0.038	9.7

[a] T_g(DSC) was also determined for Li^+/**1c** 0.25 (263.4 K) and Li^+/**1c** 2.00 (297.7 K) [Figure 1].

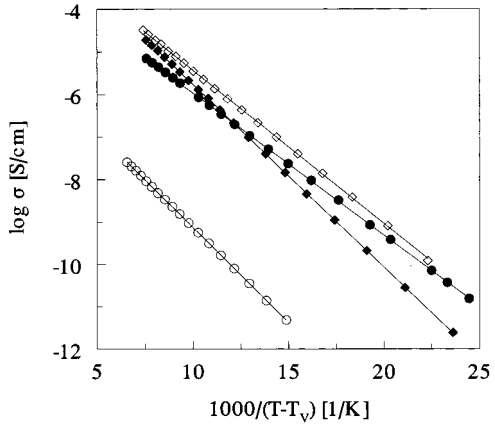

Figure 5. Log σ versus $1000/(T - T_v)$ for solid polymer electrolytes Li^+/**1a**: (○) **1a**, (●) Li^+/**1a** 0.125, (□) Li^+/**1a** 0.25, and (■) Li^+/**1a** 0.50.

electrolytes. The σ values of the Na^+/**1b** series do not increase for higher Na^+ concentrations; with respect to Na^+/**1b** 0.25 (368 K, $\sigma = 3.1 \times 10^{-6}$ S cm^{-1}) the ionic conductivity of Na^+/**1b** 0.5 is even lowered. Both the VTF and WLF parameters of the Na^+/**1b** series are listed in Table 5. Besides the occurrence of hindered cation mobility with increasing Na^+ concentration, the presence of crystalline $NaClO_4$ crystallites (WAXD measurements, see Supporting Information) for Na^+/**1b** ≥ 0.125 shows that a decrease in the effective number of charge carriers n_i is presumably responsible for the leveling off of σ.

Mobility of Polymer Chain Segments: Fine-Structure Analysis of the Apparent Activation Energy. To gain a more detailed insight in the chain segment mobility of the pristine amorphous linear poly(ether−ester)s **1a**−**c** and the effect of metal cation (Li^+ and Na^+) complexation, the dielectric relaxation spectra were subjected to an activation energy fine-structure analysis.[35] The highest temperature relaxation observed in a dielectric spectrum of an amorphous polymer is the α-relaxation peak. This peak is related to the large-scale, cooperative Brownian motion of the main chains associated with the glass−rubber transition, viz. the relaxation of the dipoles associated with this process.[33] The α-relaxation generally occurs at temperatures around and above T_g(DSC). Typically, if the dielectric experiment is performed within a frequency range from 10 to 10^5 Hz, the α-peak will correspond to T_g(DSC) + 10−20 K.[34] A more accurate method for the determination of T_g from dielectric measurements is provided by the activation energy fine-structure analysis,[35] which invokes the ratio of the derivatives of ϵ' with respect to

Table 5. VTF and WLF Conductivity-Based Fit Parameters Derived for Solid Polymer Electrolytes Na^+/1b

		VTF parameters			WLF free volume parameters				
sample	T_g(DSC) [K]	log σ_0	E_v [kJ mol^{-1}]	T_v [K]	log σ_{T_g}	C_1	C_2 [K]	$f(T_g)$	$\alpha_f \times 10^4$ [K^{-1}]
Na^+/**1b** 0.00	282.3	−2.9	8.74	241.1	−14.6	11.7	39.0	0.037	9.5
Na^+/**1b** 0.125	295.7	−0.6	8.00	253.8	−10.5	9.9	42.1	0.044	10.5
Na^+/**1b** 0.25	296.4	0.5	8.88	252.5	−10.0	10.5	44.1	0.041	9.3
Na^+/**1b** 0.50	298.7	0.7	10.32	249.5	−10.2	10.9	49.3	0.040	8.1

temperature T and the logarithm of the frequency (ln ω, eq 4):

$$E_a(\omega,T) = -RT^2 \frac{\partial\epsilon'/\partial T}{\partial\epsilon'/\partial \ln \omega} \quad (4)$$

E_a represents the apparent activation energy of the relaxation process most dominant at ω and T, ω is the applied radial frequency, and T is the temperature. The location of the maximum E_a^{max} corresponds to the glass transition temperature T_g [$T_g(E_a)$]. E_a is also related to the fractional free volume (eq 5):[36]

$$\frac{E_a(\omega,T)}{RT^2} = \frac{\alpha_f}{f(\omega,T)^2} \quad (5)$$

The "apparent" activation energy at $T = T_g$ can also be calculated from the WLF constants for conduction (eq 6):

$$E_a(C_1,C_2,T_g) = 2.303RT_g^2 \frac{C_1}{C_2} \quad (6)$$

The apparent activation energy E_a calculated, using the fine-structure analysis, from the permittivity ϵ' as a function of temperature for polymer electrolyte series Li^+/**1a**, Li^+/**1b**, and Li^+/**1c** is shown in Figure 6. As indicated by the gradual shift of the curve maxima (E_a^{max}) toward higher temperatures with increasing salt content, the T_g of each polymer electrolyte increases. These T_g values [$T_g(E_a^{max})$] are in close agreement with the T_g(DSC) values (Table 6).

For polymer electrolytes from **1a** and **1b** the apparent activation energy E_a^{max} at T_g [$T_g(E_a^{max})$] for chain segmental motion decreases with increasing salt content (Figure 6). Since E_a^{max} is related inversely to the fractional free volume (eq 5), the decrease in E_a^{max} corresponds to an increase in free volume with increasing salt content. This is in line with the free volume data derived from the conduction results using the WLF equation (Tables 2 and 3), which show that the free volume in Li^+ loaded polymers is substantially larger than in the pristine polymers. Only in the Li^+/**1c** series does E_a^{max} hardly decrease with increasing salt content; the extrapolated free volume for conduction remains roughly constant with increasing salt content. This trend agrees well with the virtually concentration-independent, fractional free volume data $f(T_g)$ for Li^+/**1c** [see WLF, eq 3 (Table 4)][37] which were calculated from the $\sigma(T)$ fits. The different quantities obtained from both the dielectric fine-structure analysis and the conductivity-based WLF data are compared in Table 6.

Dielectric Relaxation Processes in the Glassy State. In addition to the large-scale segmental relaxations (α-process) above the glass transition temperature, dielectric relaxations might also emerge in the glassy state. They originate from local (hindered) rotations involving polar groups either along the polymer main chain or in side chains.[33] These so-called secondary

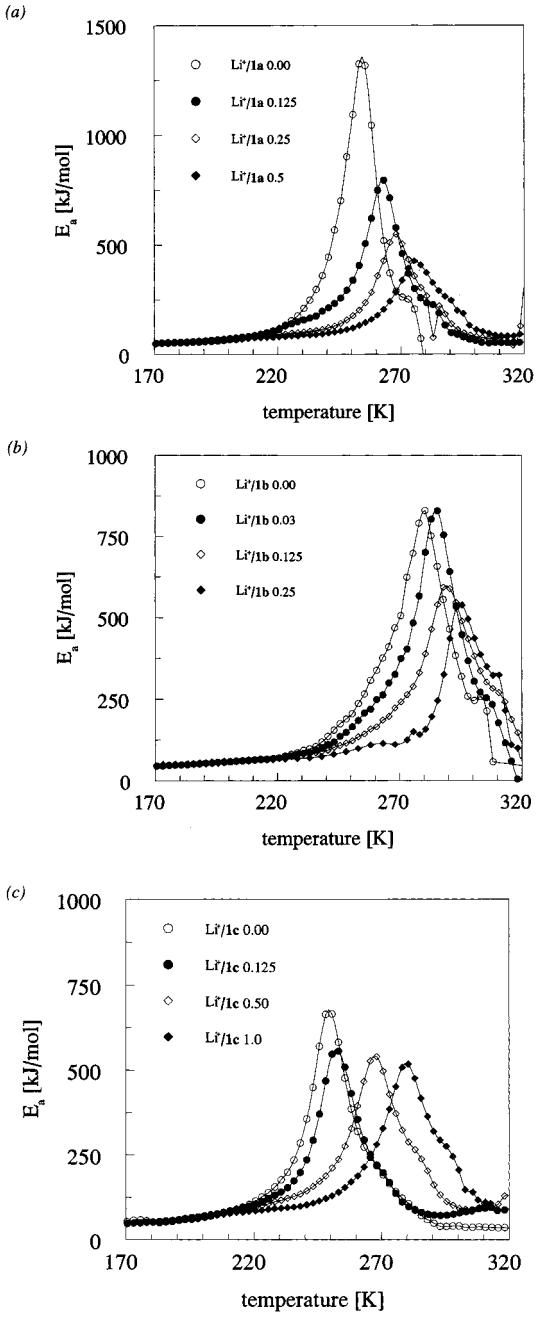

Figure 6. Local activation energy E_a calculated using the fine-structure analysis from permittivity ϵ' data at 112 Hz versus temperature for (a) Li^+/**1a**, (b) Li^+/**1b**, and (c) Li^+/**1c**.

relaxations (labeled β and γ) are due to molecular motions at the scale of a few bond lengths around a molecular dipole. Since conformational changes are mainly controlled by particular bond rotational potentials, the characteristic time is normally thermally activated; i.e., they obey an Arrhenius equation (eq 7):

$$\ln \tau = \ln \tau_0 - E_a/RT \quad (7)$$

Table 6. Comparison of T_g(DSC) with $T_g(E_a^{max})$ Obtained from an Activation Energy Fine-Structure Analysis at 112 Hz[a]

sample	T_g(DSC) [K]	$T_g(E_a^{max})$ [K]	E_a^{max} (E_a anal.) [kJ mol^{-1}]	$E_a(C_1,C_2,T_g)$ (σ-fit) [kJ mol^{-1}]	$f(T_g)/\alpha_f^{1/2}$ (E_a anal.)	$f(T_g)/\alpha_f^{1/2}$ (σ-fit)
Li^+/**1a** 0.00	253.7	254.4	1360	395	0.63	1.16
Li^+/**1a** 0.125	265.2	262.6	745	393	0.88	1.22
Li^+/**1a** 0.25	268.4	268.0	551	413	1.04	1.21
Li^+/**1a** 0.50	277.1	275.8	427	369	1.22	1.32
Li^+/**1b** 0.00	282.3	280.2	850	458	0.88	1.20
Li^+/**1b** 0.03	287.6	285.1	850	504	0.89	1.17
Li^+/**1b** 0.125	289.1	289.2	611	505	1.07	1.17
Li^+/**1b** 0.25	296.2	294.5	550	426	1.14	1.31
Li^+/**1c** 0.00	251.8	249.5	677	397	0.87	1.15
Li^+/**1c** 0.125	257.6	252.2	561	362	0.97	1.23
Li^+/**1c** 0.50	273.4	267.4	542	436	1.05	1.19
Li^+/**1c** 1.00	286.8	279.8	521	464	1.12	1.22
Na^+/**1b** 0.00	282.3	280.2	850	458	0.88	1.20
Na^+/**1b** 0.125	295.7	293.3	689	394	1.03	1.36
Na^+/**1b** 0.25	296.4	294.5	504	400	1.20	1.34
Na^+/**1b** 0.50	298.7	299.0	472	378	1.25	1.40

[a] The apparent activation energies [E_a^{max} and $E_a(C_1,C_2,T_g)$] and fractional free volume [$F(T_g)/\alpha_f^{1/2}$] calculated with the fine-structure analysis and the WLF conductivity parameters extrapolated to T_g are also given for polymer electrolytes Li^+/**1a**, Li^+/**1b**, Li^+/**1c**, and Na^+/**1b**, respectively.

In polymers **1a**−**c** two different types of polar groups are present, i.e., ester and ether moieties. In Figure 7, the dielectric loss factor tan δ ($= \epsilon''/\epsilon'$) at a frequency of 7 Hz as a function of temperature is given for the Li^+/**1a** (a), Li^+/**1b** (b), and Li^+/**1c** (c) series. For all samples the lowest temperature dielectric relaxation peak, viz. a γ-relaxation, is found at ca. 150 K[38] and possesses nearly identical peak width and position. Since the ethylene glycol moieties form the only common polar structural unit in all polymers studied, we attribute the γ-relaxation to the local twisting motion of these parts of the main chains as suggested earlier for poly(ethylene oxide) and related polymers.[39] This contention is supported by the observation that the intensity of the γ-peak decreases with increasing Li^+ content within each series. With increasing Li^+ content the number of ethylene glycol units that participate in noncovalent physical cross-linking will increase, thus reducing the number of the free ethylene glycol moieties.

In contrast, the position and peak width of the β-relaxation peak vary between and within each series. The temperature region in which this loss peak (frequency 7 Hz) is found ranges from ca. 200 to 250 K. For series Li^+/**1a** and Li^+/**1b** a clear trend is discernible; with increasing Li^+ content the β-relaxation peak is shifted to higher temperatures and increases in intensity. For the Li^+/**1c** series no such clear trend was found. However, for high salt concentrations the β-relaxation peak position becomes more or less the same for all three polymer series (∼220 K), implying a common molecular mechanism.

To gain additional information about the β-process, we studied the influence of moisture on the relaxation spectra of pristine polymer **1b**. One example is given in Figure 8 in which the temperature-dependent loss tangent of polymer **1b** after storage under ambient conditions (298 K and 65% relative humidity) for 1 week is compared with that of a sample dried prior to the measurement (see Experimental Section: Dielectric Thermal Analysis; Sample Preparation). Although the amount of physisorbed water has not been determined, the presence of moisture on the dielectric spectrum of the sample is substantial and is clearly restricted to the region of the β-relaxation. Since the γ-peak, which was attributed to local motions of the uncomplexed ethylene glycol units, remains unaffected by moisture, we conclude that the (polar) ester groups are involved in moisture absorption and thus for the sensitivity of the β-relaxation.[40]

Having established that the β-process changes with both moisture and salt concentration, we undertook a quantitative analysis of the intensity as well as the activation parameters (E_a, τ_0) of the secondary relaxations. For this purpose a novel fit technique was applied,[41] which allows the simultaneous fit of the dielectric loss ϵ'' in both the frequency and temperature domain by minimizing (eq 8):

$$\sum_{\omega_0}^{\omega_0+n\Delta\omega} \sum_{T_0}^{T_0+m\Delta T} (\epsilon''_m - \epsilon'')^2 \qquad (8)$$

where $\epsilon''_m(\omega,T)$ is the measured loss and $\epsilon''(\omega,T)$ the theoretical loss. Since secondary relaxations are typically broad and symmetric, a symmetric relaxation function (Cole−Cole function), with the parameters relaxation strength $\Delta\epsilon$, broadness parameter a ($0 < a < 1$), and relaxation time $\tau(T)$, was selected (eq 9):

$$\epsilon^*(\omega) = \epsilon' - i\epsilon'' = \epsilon_\infty + \frac{\Delta\epsilon(T)}{1 + (i\omega\tau(T))^a} \qquad (9)$$

in which $\Delta\epsilon$ is weakly dependent on temperature. To fit the loss data given in Figures 7 and 8, we combined two Cole−Cole relaxation functions each described by its own set of Arrhenius parameters. A more detailed description of this technique can be found in ref 40. The results of the 2D fit procedure are given in Tables 7 and 8. As expected, the γ-relaxation appears to be almost insensitive to moisture and salt concentration; its activation parameters ($E_a = 0.38$ eV, $\log \tau_0 = -14.8$) and low Cole−Cole exponent of $a = 0.33$ are typical for a broad and "truly" thermally activated relaxation process.

The β-relaxation, however, shows the tendency to increase in strength acompanied with changes in τ_0 by orders of magnitude (**1b**) depending on the Li^+ concentration. We further note that the relaxation strength $\Delta\epsilon$ of the β-process given in Tables 7b and 8b increases significantly with increasing water content and Li^+ concentration. These facts together with the unusually strong variation in the activation parameters suggest

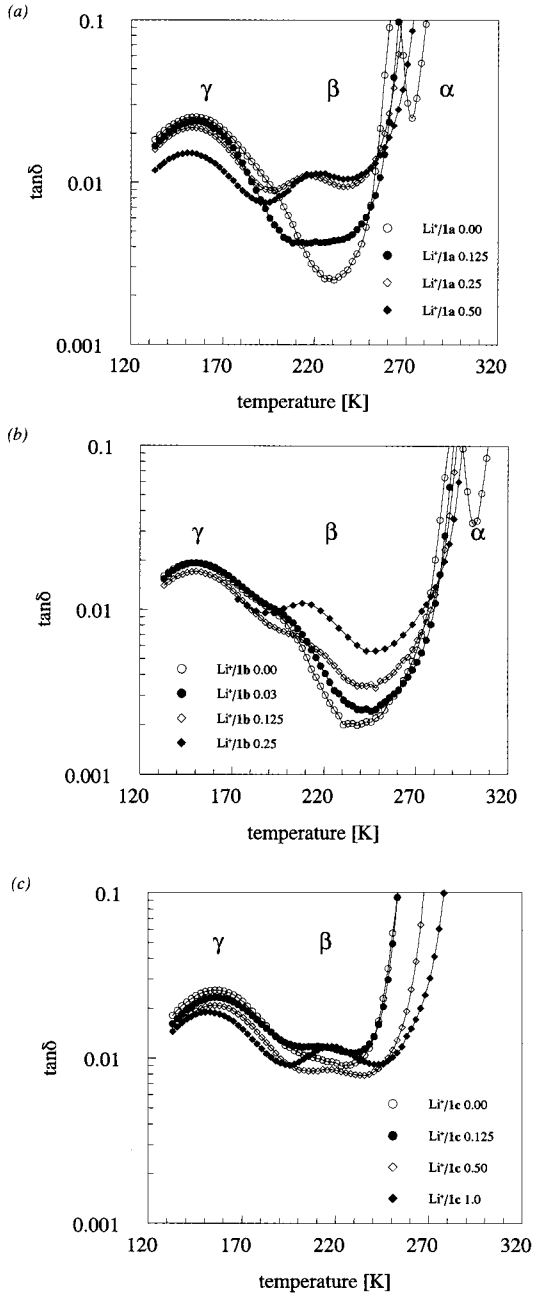

Figure 7. Dielectric loss factor tan δ versus temperature at a frequency of 7 Hz for (a) Li^+/**1a**, (b) Li^+/**1b**, and (c) Li^+/**1c**.

that there are two different β-processes, which virtually overlap each other. Consequently, the sensitivity to moisture may be explained by the role of hydrophilic ester groups causing a specific relaxation process β_1.[40] On the other hand, the increase in the observed β-relaxation strength with increasing Li^+ content could originate from an additional second β-process (β_2) involving the ethylene glycol/Li^+ coordination complexes.

We have worked out the latter idea in more detail. For Li^+ cations it is well established that four oxygen atoms may coordinate with Li^+ in a tetrahedral arrangement. For polymers **1a**−**c** this situation can easily be reached by complexing two pairs of adjacent ether groups provided by the same or by two different polymer chains. Once locked in a tetrahedral configuration, even small rotations of these ether groups manifested by the γ-relaxation will be inhibited. Another feature of the

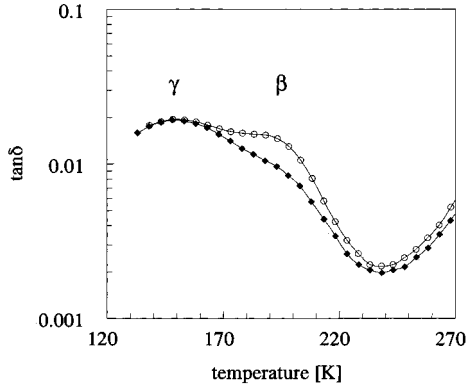

Figure 8. Dielectric loss factor tan δ versus temperature at a frequency of 7 Hz for pristine **1b** (○) after storage at ambient temperature (measured from 123 to 323 K) and (■) after cooling down from 323 K (measured from 323 to 123 K) (see Experimental Section: Dielectric Thermal Analysis; Sample Preparation).

Table 7. Activation Parameters E_a, Broadness Parameter a, and Relaxation Strength $\Delta\epsilon$ of the γ- (a) and of the β-Relaxation (b) of Polymer Electrolytes Li^+/1b[a]

sample	E_a [kJ mol^{-1}]	log τ_0	$\Delta\epsilon$ CC fit	$\Delta\epsilon_{\beta 2}$ Onsag.	a
		(a) γ-Relaxation			
dry samples					
Li^+/**1b** 0.00	37 ± 1	−15.0 ± 0.2	0.55		0.33
Li^+/**1b** 0.03	37 ± 1	−14.9 ± 0.2	0.54		0.33
Li^+/**1b** 0.125	37 ± 1	−14.8 ± 0.2	0.49		0.31
Li^+/**1b** 0.25	37 ± 5	−14.6 ± 1.4	0.45		0.32
wet samples					
Li^+/**1b** 0.00	37 ± 1	−15.0 ± 0.2	0.57		0.33
Li^+/**1b** 0.125	35 ± 1	−14.2 ± 0.2	0.65		0.33
		(b) β-Relaxation			
dry samples					
Li^+/**1b** 0.00	57 ± 1	−16.9 ± 0.2	0.11	0	0.49
Li^+/**1b** 0.03	57 ± 2	−16.6 ± 0.5	0.13	0.02	0.44
Li^+/**1b** 0.125	46 ± 1	−12.8 ± 0.3	0.08	0.08	0.53
Li^+/**1b** 0.25	52 ± 2	−14.4 ± 0.4	0.15	0.17	0.50
wet samples					
Li^+/**1b** 0.00	56 ± 1	−16.6 ± 0.3	0.16	0	0.55
Li^+/**1b** 0.125	51 ± 1	−14.8 ± 0.2	0.28	0.08	0.51

[a] See Experimental Section: Dielectric Thermal Analysis; Sample Preparation.

Table 8. Activation Parameters E_a, Broadness Parameter a, and Relaxation Strength $\Delta\epsilon$ of the γ- (a) and of the β-Relaxation (b) of Polymer Electrolytes Li^+/1a[a]

sample	E_a [kJ mol^{-1}]	log τ_0	$\Delta\epsilon$	$\Delta\epsilon_{\beta 2}$ Onsag.	a
	(a) γ-Relaxation (Dry Samples)				
Li^+/**1a** 0.00	39 ± 1	−15.3 ± 0.2	0.80[b]		0.35[b]
Li^+/**1a** 0.125	41 ± 2	−15.5 ± 0.2	0.59[b]		0.33[b]
Li^+/**1a** 0.25	38 ± 1	−14.9 ± 0.2	0.67[b]		0.33[b]
Li^+/**1a** 0.50	37 ± 1	−14.6 ± 0.2	0.37[b]		0.32[b]
	(b) β-Relaxation (Dry Samples)				
Li^+/**1a** 0.00	71 ± 4	−21.0 ± 1.4	0.18[c]	0	0.33
Li^+/**1a** 0.125	56 ± 4	−14.3 ± 1.0	0.06[c]	0.09	0.38
Li^+/**1a** 0.25	56 ± 2	−14.9 ± 0.5	0.17[c]	0.17	0.52
Li^+/**1a** 0.50	57 ± 2	−15.0 ± 0.4	0.14[c]	0.35	0.47

[a] See Experimental Section: Dielectric Thermal Analysis; Sample Preparation. [b] At 173 K. [c] CC fit.

tetrahedral is illustrated in Figure 9a, which shows a Li^+/dimethylethylene glycol model complex after geometry optimization using the MMX force field.[42] As expected, the strong partial dipole moments of the four ether groups (each with a dipole moment μ = 1.14 D) effectively cancel;[43] i.e., the rigid complex is apolar. The existence of a "local" relaxation process which strength

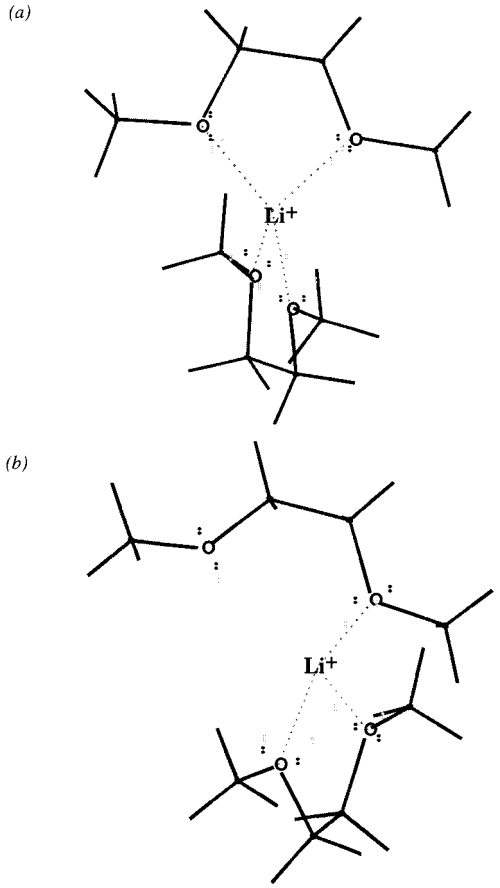

Figure 9. MMX optimized structure of a model complex of Li^+/dimethylethylene glycol: (a) coordination of Li^+ by four oxygens and (b) Partially (de)complexed Li^+ cation.

is proportional to the number of Li^+/polymer complexes leads to the conclusion that temporary breaking up and remaking of at least one coordination bond is the most likely origin for the β_2-relaxation process (Figure 9b).

Relaxation processes involving temporary chemical bonds are known as "chemical relaxations" and have also been observed in H-bonded physical networks[44] above the glass transition temperature. The most prominent feature of a (dielectric) chemical relaxation in contrast to a normal rotational dipole relaxation is that its thermal activation is determined by the strength of the specific physical bonds involved rather than by a potential barrier. We have related the experimentally determined relaxation strength $\Delta\epsilon = \epsilon_s - \epsilon_\infty$ of the β-process to the molecular dipole moment μ and the concentration of Li^+ complexes by using the Onsager equation (eq 10):

$$\frac{g\mu^2 n N_A \rho}{\bar{M}_w} = \frac{9kT\epsilon_0(\epsilon_s - \epsilon_\infty)(2\epsilon_s + \epsilon_\infty)}{\epsilon_s(\epsilon_\infty + 2)^2} \qquad (10)$$

in which M_w, N_A, ρ, n, and g denote the molecular mass of the repeat unit, Avogadro's number, the density, the number of Li^+ complexes per repeat unit, and the Kirkwood correlation factor. From eq 10 the relevant dipole moment μ is the only unknown parameter. (We have set $g = 1$, viz. neglecting correlations between different complexes.) To get an estimate for μ of a partially broken complex, we performed a second model calculation (Figure 9b). Due to the simplifications made, the dipole moment μ of 1.2 D is not correct, but it will be of the proper order of magnitude. Inserting the parameters $M_w = 534$ (repeat unit of **1a**) or $M_w = 554$ (repeat unit of **1b**), $n = 0-1$, $\rho = 1000$ kg/m^3,and $\epsilon_\infty = 3$, and solving eq 10 for ϵ_s yields the $\Delta\epsilon_{\beta 2\text{Onsag.}}$ values listed in Tables 7 and 8.

By comparison with the fitted relaxation strength, a good agreement with the theoretical predicted $\Delta\epsilon$ data can be seen, in particular for polymer **1b** and for Li^+/**1b** with high salt concentrations. This supports the proposed "chemical relaxation" mechanism for the β_2-process.

Clearly, the effect of the anions requires further investigations. To gain insight in the anion contributions instead of $LiClO_4$, other salts such as $LiCF_3SO_3$ and LiSCN will have to be used; experiments are in progress.

Conclusions

The readily accessible, amorphous polymers **1a**, **1b**, and **1c**, which contain bis(1,4,7-trioxanonyl) (triethylene glycol) segments in their main chain, represent novel ion-conducting matrices. Despite the fact that only triethylene glycol segments are present, ion conductivities of $\sigma = 3.2 \times 10^{-5}$ S cm^{-1} at 368 K are found for Li^+/**1a**. By increasing the number of ethylene glycol units in the total main chain structure, which is done in polymer **1c**, the ionic conductivity is even raised to $\sigma = 1 \times 10^{-4}$ S cm^{-1} at 368 K. These results hold a promise for the development of related linear polymers possessing even higher conductivities at lower temperatures. For all polymer electrolytes the conductivity $\sigma(T)$ above T_g obeys a Vogel−Tammann−Fulcher (VTF) relation in a wide temperature range ($T_g + 5$ K $\leq T \leq T_g + 100$ K). A similar temperature dependence was found for the relaxation time $\tau(T)$ of the α-relaxation (Li^+/**1a** 0.123). This proves that the free volume controls both ionic conduction and the relaxation behavior of the chain segments.

By means of a fine structure analysis of the activation energy, the dielectric α-process around the glass transition for **1a**−**c** and **1b** was closely studied in the absence and presence of dissolved $LiClO_4$ and $NaClO_4$, respectively. From the most prominent peak in the apparent activation energy spectra T_g was determined and found to agree well with T_g(DSC) values. Furthermore, the fractional free volume at T_g was assessed. It shows an increase of $f(T_g)$ with an increasing amount of dissolved salt in particular for polymers **1a,b**. Dielectric spectroscopy at temperatures below T_g revealed the presence of three secondary relaxations (γ, β_1, β_2), of which β_1 and β_2 almost coincide. The β_1-relaxation is in particular observed in salt-free and weakly complexed samples that had been exposed to ambient humidity, suggesting a local motion involving the ester moieties. The two other relaxations were assigned to local motions involving either free (γ) or coordinated (β_2) EO sequences, resulting in a decrease or increase of the relaxation strength with salt concentration. Molecular modeling supports the idea that the β_2 process arises from temporary breaking up and remaking of at least one O−Li^+ coordination bond within the tetrahedral polymer−cation complex (chemical relaxation). This suggests that the lifetime of the polymer/Li^+ complex as a whole must be of the order of the β_2-relaxation time. It is therefore likely that the cationic mobility $\mu^+(T)$ is triggered by the (thermally activated) β_2-process. For

$T > T_g$ the overall ionic conductivity σ follows a VTF relation, i.e., is controlled by free volume relaxation.

Experimental Section

General. NMR spectra were recorded on a Bruker AC 300 spectrometer at 300.13 (^{1}H) and 75.47 MHz (^{13}C) using the solvent as internal standard. IR spectra were measured either on a Mattson Galaxy series FT-IR 5000 spectrophotometer using a diffuse reflection accessory or a dispersive Perkin-Elmer 283 spectrophotometer. Molecular weight distributions were determined with size exclusion chromatography [Thermo Separation Products Spectra series P200, Shodex Standard KF-804 column, eluent THF, UV detection (λ 254 nm), reference polystyrene standards]. Thermal properties were determined with differential scanning calorimetry (Mettler DSC12-E, temperature range 233−473 K; heating and cooling rate 5 and 2 K min^{-1}, respectively) and thermogravimetry [TGA(N_2), Perkin-Elmer TGS-2 with an autobalance AR-2, temperature range 323−1123 K, heating rate 20 K min^{-1}]. Wide-angle X-ray powder diffraction (WAXD) analyses were performed with a Nonius PDS 120 powder diffractometer system equipped with a position sensitive detector of 120° 2θ, using Co Kα_1 (λ = 1.788 97 Å) radiation. Polymer films were prepared on aluminum plates at elevated temperatures in a dry N_2 atmosphere. Elemental analysis was carried out by H. Kolbe Mikroanalytisches Laboratorium Mülheim a.d. Ruhr, Germany. **Caution:** solid polymer electrolytes containing $LiClO_4$ should be handled with care due to potential explosion danger.

Dielectric Thermal Analysis; Equipment and Methods. Dielectric measurements were performed with a broadband dielectric spectrometer (Solartron 1260 frequency response analyzer for frequencies from 10^{-2} Hz to 1 kHz and a Hewlett-Packard 4284A LCR meter for frequencies between 1 kHz and 1 MHz) using parallel plates. The use of a sinusoidal voltage has the advantage that the ion conductivity of the bulk of a sample is determined. Ionic conductivities σ (S cm^{-1}) were determined by fitting of up to two relaxation functions and a (ohmic) conduction term to the complex permittivity ϵ^* measured in the frequency range of 0.1 Hz and 100 kHz and the temperature range of 123−373 K.

Dielectric Thermal Analysis; Sample Preparation. Dielectric spectroscopy measurements were done using aluminum parallel plate electrodes (upper electrode, diameter 20 mm; bottom electrode, diameter 30 mm) of homogeneous thickness. The polymeric material (100−150 mg) was placed on the bottom electrode and heated to ca. 373 K under a dry N_2 atmosphere. When the material became fluidlike, it was spread out over an area of ca. diameter 20 mm. After putting at least three spacers (quartz fibers, thickness 50 ± 2 μm) on top of the polymer layer, the upper electrode was pressed onto the polymer layer at an elevated temperature (373 K). The thickness of the polymer layers was verified by means of a Nikon MUC-151 thickness meter. The dielectric experiments were performed under dry N_2 gas and, with the exception of the wet samples, were always carried out during slow cooling (rate <1 K min^{-1}) starting from 413 K in order to remove any physisorbed water. The wet samples obtained after exposure to ambient conditions (298 K, 65% relative humidity) for 1 week, which results in a water uptake of ca. 5%, were initially cooled from 289 to 133 K and subsequently heated to 393 K.

Solid Polymer Electrolytes. Solid polymer electrolytes were prepared by mixing THF solutions of **1a**−**c** with THF solutions of either $LiClO_4$ or $NaClO_4$ (**1b**, see text) followed by slow evaporation of the solvent under a stream of dry N_2. Any remaining traces of solvent were removed by drying the samples in vacuo (10^{-2} Torr) at 393 K. For different loadings of dissolved $LiClO_4$ and $NaClO_4$ different ratios of moles of cation per mole of polymer repeat unit were used. Note that due to differences in polymer chain architecture the salt concentration 1.0 for **1a,b** corresponds to 10 oxygen atoms (8 ether-like and 2 ester-like) per cation, whereas for **1c** at the same ratio 14 oxygen atoms (12 ether-like and 2 ester-like) are available per cation. All samples were prepared and stored under a dry N_2 atmosphere.

Syntheses. *3,6,9,12-Tetraoxadecatetradecane Bis-Acid Chloride (**3c**).*[45] To a cooled suspension (0 °C) of NaH (12.49 g, 0.52 mol) in dry THF (250 mL) a solution containing both freshly distilled triethylene glycol (30.8 g, 0.20 mol) and methyl bromoacetate (78.6 g, 0.51 mol) in THF (40 mL) was slowly added within 3 h. During the addition the temperature of the reaction mixture was kept below 10 °C. Subsequently, the reaction mixture was stirred at room temperature for another 24 h, after which CH_3OH (50 mL) was carefully added to destroy excess NaH. After filtration of the reaction mixture the filtrate was concentrated under reduced pressure to give a viscous brown oil which was extracted with diethyl ether (3 × 500 mL) to yield crude 3,6,9,12-tetradecanoic acid dimethyl ester (57 g) as a yellow oil. Distillation under reduced pressure [148−156 °C (0.01 mmHg)] afforded 22.2 g (75 mmol, 37%) of pure 3,6,9,12-tetradecanoic acid dimethyl ester as a colorless oil. ^{1}H NMR ($CDCl_3$): δ 4.15 (s, 4H), 3.73 (s, 6H), 3.71−3.65 (m, 8H), and 3.64 (s, 4H) ppm. ^{13}C NMR ($CDCl_3$): δ 170.80, 70.90, 70.63, 70.56, 68.60, and 51.70 ppm. IR (NaCl) 2960−2880, 1760, 1440, 1130, 850, and 700 cm^{-1}. All spectroscopic data were in agreement with those previously reported.[45] The dimethyl ester was converted into **3c** using the following procedure. A solution of the dimethyl ester (3.82 g, 13 mmol) in aqueous NaOH (1.11 g, 28 mmol in 10 mL of H_2O) was heated at reflux temperature for 1 h. After cooling to room temperature the turbid reaction mixture was washed with CH_2Cl_2 (3 × 10 mL) to remove any unreacted organic material. Freeze-drying of the remaining yellow oil under reduced pressure afforded 4.06 g (13 mmol) of the bis-sodium salt as a light yellow solid. Under a dry N_2 atmosphere dry diethyl ether (10 mL), excess oxalyl chloride (4 mL), and a small amount of DMF (100 μL) were added to the bis-sodium salt. After 6 h a second portion of oxalyl chloride (4 mL) was added. When the gas evolution ceased, the reaction mixture was diluted with dry diethyl ether (50 mL) and centrifuged to separate any insoluble material. The supernatant was concentrated under reduced pressure to afford 3.59 g (11.8 mmol, 90%) of **3c** as a brownish oil. ^{1}H NMR ($CDCl_3$): δ 4.50 (s, 4H), 3.79−3.76 (m, 4H), 3.70−3.67 (m, 4H), and 3.64 (s, 4H) ppm. ^{13}C NMR ($CDCl_3$): δ 172.0, 76.6, 71.3, 70.7, and 70.6 ppm. IR (NaCl) 2920−2880, 1810, 1460, 1415, 930, and 750 cm^{-1}. All spectroscopic data of **3c** were in agreement with those previously reported.[45]

General Procedure for Melt Polycondensation. Equimolar amounts of diol **2** (5 mmol) and each of the diacid chlorides **3a**−**c** (5 mmol) were mixed in a Schlenk vessel. The temperature of the mixture was initially maintained at 373 K under dynamic vacuum for the removal of evolving HCl(g).[11] When the mixture became too viscous to enable magnetic stirring, the reaction was forced to completion by increasing the temperature to 453 K for 20 min, with the exception of the melt condensation of **1c** due to the thermal instability of the incorporated bis-acid chloride component **3c** (see text). After cooling to room temperature the crude polymer was dissolved in THF and reprecipitated in a 5-fold excess of vigorously stirred CH_3OH. **1a**;[11] yield 75%. ^{1}H NMR ($CDCl_3$): δ 7.85 (d, 2H, ^3J = 8.5 Hz), 7.33 (t, 2H, ^3J = 7.9 Hz), 6.83 (d, 2H, ^3J = 7.6 Hz), 4.29−4.26 (m, 4H), 4.23−4.20 (m, 4H), 3.99−3.94 (m, 4H), 3.80−3.77 (m, 4H), 3.72−3.66 (m, 8H), 2.32−2.28 (m, 4H), 1.65−1.60 (m, 4H) ppm. ^{13}C NMR ($CDCl_3$): δ 173.1, 154.3, 126.8, 125.1, 114.6, 105.7, 70.9, 70.6, 69.8, 69.2, 67.9, 63.4, 33.7, and 24.2 ppm. IR (KBr) 3060, 2947, 2883, 1741, 1273, 1143, and 787 cm^{-1}. Anal.Calcd for $(C_{28}H_{38}O_{10})_n$: C, 62.91; H. 7.17. Found: C, 62.84; H, 7.13. See also Table 1. **1b**;[11] yield 65%. ^{1}H NMR ($CDCl_3$): δ 8.07 (s, 4H), 7.83 (d, 2H, ^3J = 8.5 Hz), 7.31 (t, 2H, ^3J = 7.9 Hz), 6.79 (d, 2H, ^3J = 7.6 Hz), 4.49−4.46 (m, 4H), 4.27−4.24 (m, 4H), 3.99−3.96 (m, 4H), 3.86−3.72 (m, 12H) ppm. ^{13}C NMR ($CDCl_3$): δ 165.7, 154.3, 133.9, 129.6, 126.7, 125.0, 114.6, 105.6, 71.0, 70.7, 69.8, 69.1, 67.8, and 64.4 ppm. IR (KBr) 3088, 2893, 1728, 1278, 1111, and 787 cm^{-1}. Anal. Calcd for $(C_{30}H_{34}O_{10})_n$: C, 64.97; H, 6.18. Found: C, 64.85; H, 6.20. See also Table 1. **1c**; yield 80%. ^{1}H NMR (DMSO-d_6): δ 7.72 (d, 2H, ^3J = 8.4 Hz) 7.37 (t, 2H, ^3J = 8.0 Hz), 6.97 (d, 2H, ^3J = 7.5 Hz) 4.23 (m, 4H), 4.15−4.18 (m, 4H), 4.10 (s, 4H), 3.87 (m, 4H), 3.65−3.54 (m, 12H), 3.57−3.47 (m,

8H), and 3.47 (s, 4H) ppm. ^{13}C NMR (DMSO-d_6): δ 170.0, 153.7, 125.9, 125.2, 113.7, 105.8, 69.9, 69.8, 69.7, 69.5 (2×), 68.9, 68.1, 67.6, 67.5, and 63.2. IR (KBr): 3090, 3070, 2960−2840, 1760, 1600, 1510, 1460, 1420, 1270, 1200, 1080, 970, 850, and 775 cm^{-1}. Anal. Calcd for $(C_{32}H_{46}O_{14})_n$: C, 58.71; H, 7.08. Found: C, 58.65; H, 7.01. See also Table 1.

Supporting Information Available: Three figures, viz. TGA(N_2) curves of Poly(ether−ester)s **1a** and **1c**, T_g(DSC) versus $NaClO_4$ concentration for solid polymer electrolytes Na^+/**1b** and wide-angle X-ray diffraction pattern of (a) **1b** and (b) Na^+/**1b** 1.0. This material is available free of charge via the Internet at http://pubs.acs.org.

References and Notes

(1) For a review, see: Ratner, M. A.; Shriver, D. F. *Chem. Rev.* **1988**, *88*, 109.
(2) Murata, K. *Electrochim. Acta* **1995**, *40*, 2177.
(3) Andrei, M.; Roggero, A.; Marchese, L.; Passerini, S. *Polymer* **1994**, *35*, 3592.
(4) Doeff, M. M.; Visco, S. J.; Ma, Y.; Peng, M.; Ding, L.; De Jonghe, L. C *Electrochim. Acta* **1995**, *40*, 2205.
(5) Druger, S. D.; Nitzan, A.; Ratner, M. *J. Chem. Phys.* **1983**, *79*, 3133.
(6) Fenton, D. E.; Parker, J. M.; Wright, P. V. *Polymer* **1973**, *14*, 589.
(7) Armand, M. B.; Chabagno, J. M.; Duclot, M. J. In *Fast Ion Transport in Solids*; Vashishta, P., Mundy, J. N., Shenoy, G. K., Eds.; North-Holland: Amsterdam, The Netherlands, 1979; p 131.
(8) Florjanczyk, Z.; Krawiec, W.; Wieczorek, W.; Siekierski, M. *J. Polym. Sci. B* **1995**, *33*, 629.
(9) Le Nest, J.-F.; Gandini, A.; Cheradame, H. *Br. Polym. J.* **1988**, *20*, 253.
(10) Hawker, C. J.; Chu, F.; Pomery, P. J.; Hill, D. J. T. *Macromolecules* **1996**, *29*, 3831.
(11) Mertens, I. J. A.; Jenneskens, L. W.; Wentzel, B. B.; Wübbenhorst, M.; Van Turnhout, J. *Acta Polym.* **1997**, *48*, 314.
(12) Ballauf, M. *Makromol. Chem., Rapid Commun.* **1986**, *7*, 407.
(13) Mertens, I. J. A.; Jenneskens, L. W.; Vlietstra, E. J.; Van der Kerk-van Hoof, A. C.; Zwikker, J. W.; Smeets, W. J. J.; Spek, A. L. *J. Chem. Soc., Chem. Commun.* **1995**, 1621. Mertens, I. J. A.; Wegh, R.; Jenneskens, L. W.; Vlietstra, E. J.; Van der Kerk-van Hoof, A. C.; Zwikker, J. W.; Cleij, T. J.; Smeets, W. J. J.; Veldman, N.; Spek, A. L. *J. Chem. Soc., Perkin Trans. 2* **1998**, 725.
(14) Considerable molecular weights are found. See also: Ignatova, M.; Manolova, N.; Rashkov, I. *Macromol. Chem. Phys.* **1995**, *196*, 2695.
(15) Despite the increased flexibility of the bis-acid chloride **3c**, T_g(DSC) of **1c** is not lowered compared to that of **1a**. It is anticipated that residual NaCl, derived from the synthesis of **3c**, is responsible for the elevated T_g, due to physical interchain cross-linking.
(16) Slopes of -2.80×10^{-4} dm^3 mol^{-1} K^{-1}, -2.77×10^{-4} dm^3 mol^{-1} K^{-1}, and -3.12×10^{-4} dm^3 mol^{-1} K^{-1} are obtained using a density d of **1a**−**c** equal to 1 kg dm^{-3}. With $d = 0.9$ and 1.1 kg dm^{-3} the slopes are -3.11×10^{-4} dm^3 mol^{-1} K^{-1}, -3.09×10^{-4} dm^3 mol^{-1} K^{-1}, and -3.47×10^{-4} dm^3 mol^{-1} K^{-1}, and -2.54×10^{-4} dm^3 mol^{-1} K^{-1}, -2.52×10^{-4} dm^3 mol^{-1} K^{-1}, and -2.85×10^{-4} dm^3 mol^{-1} K^{-1}, respectively.
(17) *Natl. Bur. Stand. (U.S.), Circ. 539* **1957**, *7*, 49.
(18) Braekken, H. *Kristallogr., Kristallgeom., Kristallphys., Kristallchem.* **1930**, *75*, 539.
(19) Lin, L.; Cates, E.; Bianconi, P. A. *J. Am. Chem. Soc.* **1994**, *116*, 4738.
(20) Bruce, P. G. *Electrochim. Acta* **1995**, *40*, 2077.
(21) MacDonald, J. R. *Impedance Spectroscopy: Emphasizing Solid Materials and Systems*; Wiley: New York, 1987.
(22) Since the T_g of **1b** is positioned 30 K above that of **1a**, a fairer comparison is given by data of salt/polymer series **1b** at 398 K with that of **1a** at 368 K.
(23) Bannister, D. J.; Davies, G. R.; Ward, I. M.; McIntyre, J. E. *Polymer* **1984**, *25*, 1600.
(24) Manoravi, P.; Selvaraj, I. I.; Chandrasekhar, V.; Shahi, K. *Polymer* **1993**, *34*, 1339.
(25) Nicholas, C. V.; Wilson, D. J.; Booth, C.; Giles, J. R. M. *Br. Polym. J.* **1988**, *20*, 289.
(26) Wieczorek, W.; Zalewska, A.; Raducha, D.; Florjanczyk, Z.; Stevens, J. R.; Ferry, A.; Jacobsson, P. *Macromolecules* **1996**, *29*, 143.
(27) Vogel, H. *Z. Phys.* **1921**, *22*, 645. Tammann, G.; Hesse, G. *Z. Anorg. Allg. Chem.* **1926**, *156*, 245. Fulcher, G. S. *J. Am. Ceram. Soc.* **1925**, *8*, 339.
(28) Miyamoto, T.; Shibayama, K. *J. Appl. Phys.* **1973**, *44*, 5372.
(29) The mean relaxation time of the α-relaxation τ_α has been determined by fitting the $\epsilon'(\omega)$ and $\epsilon''(\omega)$ spectra with a combination of an asymmetric Havriliak−Negami function and an ohmic conduction term. This technique is restricted to moderately conducting samples in which the dipolar loss is not overshadowed by conduction or electrode polarization.
(30) Wübbenhorst, M.; Mertens, I. J. A.; Jenneskens, L. W.; van Turnhout, J. Manuscript in preparation.
(31) Doolittle, A. K. *J. Appl. Phys.* **1951**, *22*, 1471; **1952**, *23*, 236.
(32) Williams, M. L.; Landel, F.; Ferry, J. D. *J. Am. Chem. Soc.* **1955**, *77*, 3701.
(33) Simon, G. P. *Mater. Forum* **1994**, *18*, 235.
(34) DSC measurements should be related to dielectric analysis measurements at 10^{-3} Hz.
(35) Wübbenhorst, M.; Van Koten, E.; Jansen, J.; Mijs, W.; Van Turnhout, J. *Macromol. Rapid Commun.* **1997**, *18*, 139. Steeman, P. A. M.; Van Turnhout, J. *Macromolecules* **1994**, *27*, 2364.
(36) For a review (in Dutch): Van Turnhout, J. In *Kunststoffen 1986−Terugblik en toekomst*; Brüggemann, H. M., Ed.; Wijt: Rotterdam, The Netherlands, 1986; p 285.
(37) If conduction contributes considerably to the dielectric losses ϵ'', the free volume for conduction can be derived from a similar equation as eq 5, i.e., $(\partial\epsilon''/\partial T)/[\partial\epsilon''/\partial(\ln\omega)] = -\alpha_f/f(T)^2$.
(38) A similar interpretation was given for polybibenzoates containing ethylene glycol spacers from a dynamical mechanical analysis: Heaton, N. J.; Benavente, R.; Pérez, E.; Bello, A.; Pereña, J. M. *Polymer* **1996**, *37*, 3791.
(39) Ishida, Y.; Matsuo, M.; Takayanagi, M. *J. Polym. Sci., B* **1965**, *3*, 321.
(40) For polyamides and polyurethanes a similar strong sensitivity to moisture was found for the β-relaxation process. For an overview, see: McCrum, N. G.; Read, B. E.; Williams, G. *Anelastic and Dielectric Effects in Polymeric Solids*; Dover Publications: New York, 1991.
(41) Boersma, A.; Van Turnhout, J.; Wübbenhorst, M. *Macromolecules* **1998**, *31*, 7453.
(42) PCMODEL: MMX force field; Serena Software, Bloomington, IN, 1990.
(43) A close to tetrahedral geometry was obtained using the MMX force field implemented in PCMODEL.[42]
(44) Müller, M.; Seidel, U.; Stadler, R. *Polymer* **1995**, *36*, 3143.
(45) Miyazaki, M.; Shimoishi, Y.; Miyata, H.; Tôei, K. *J. Inorg. Nucl. Chem.* **1974**, *36*, 2033.

MA981901J